SANDIA REPORT
SAND2021-11937
Printed Click to enter a date

Sandia National Laboratories

A Fast-Cycle Charge Noise Measurement for Better Qubits

Rupert Lewis, Will Kindel, Sueli Skinner-Ramos, and Tom Harris

Prepared by
Sandia National Laboratories
Albuquerque, New Mexico
87185 and Livermore,
California 94550

Issued by Sandia National Laboratories, operated for the United States Department of Energy by National Technology & Engineering Solutions of Sandia, LLC.

Available to DOE and DOE contractors from
U.S. Department of Energy
Office of Scientific and Technical Information
P.O. Box 62
Oak Ridge, TN 37831

Telephone: (865) 576-8401
Facsimile: (865) 576-5728
E-Mail: reports@osti.gov
Online ordering: http://www.osti.gov/scitech

Available to the public from
U.S. Department of Commerce
National Technical Information Service
5301 Shawnee Rd
Alexandria, VA 22312

Telephone: (800) 553-6847
Facsimile: (703) 605-6900
E-Mail: orders@ntis.gov
Online order: https://classic.ntis.gov/help/order-methods/

ABSTRACT

Defects in materials are an ongoing challenge for quantum bits, so called qubits. Solid state qubits—both spins in semiconductors and superconducting qubits—suffer from losses and noise caused by two-level-system (TLS) defects thought to reside on surfaces and in amorphous materials. Understanding and reducing the number of such defects is an ongoing challenge to the field.

Superconducting resonators couple to TLS defects and provide a handle that can be used to better understand TLS. We develop noise measurements of superconducting resonators at very low temperatures (20 mK) compared to the resonant frequency, and low powers, down to single photon occupation.

ACKNOWLEDGEMENTS

We thank the New Ideas committee for funding this research. A portion of this research was carried out at the Center for Integrated Nanotechnologies Integration Lab. We thank John Nogan and the rest of the CINT support staff for their assistance.

We also thank Eric Shaner for allowing us the use of a 1K refrigerator and Robert Schoelkopf for the gift of the dilution fridge used in these measurements.

CONTENTS

LIST OF FIGURES

LIST OF TABLES

This page left blank

ACRONYMS AND DEFINITIONS

Abbreviation	Definition
TLS	two level systems
SC	superconductor
CPW	co-planar waveguide
cQED	circuit quantum-electrodynamics
fwhm	full width at half maximum

1. INTRODUCTION

The central idea of this project is to use the sensitivity of a high-quality factor (Q) resonator to track defects in materials used for solid state qubits. Solid state qubits are principally of two types. The first qubit type is realized with the spin of an electron or hole or even an atomic nucleus (spin qubits) which can be isolated in a quantum dot [1]. Spin qubits are confined and manipulated by gates and addressed by rf signals. Superconducting qubits (SC qubits) are the other principle type of solid state qubit and have grown in popularity over the past decade as they are easy to make and have coherence times comparable to that of confined electron spins. SC qubits are currently limited in coherence time by defects which couple to electric fields generated within the qubit [2]. What both these types of solid state qubits share is being built upon a semiconductor substrate, usually silicon, with subsequent metal depositions to define the qubit. Deposition of materials necessarily include at least the substrate-to-metal interface and the metal-to-vacuum interface. More complex designs require more metal depositions and so involve insulators between the metals. In short, all solid state qubits include multiple materials interfaces where defects can reside.

The semiconductor industry is not a stranger to defects at surfaces and in amorphous oxides. Indeed, many books have been written on the subject [3]. However, analog and digital semiconductor devices face less stringent requirements and are more tolerant of defects than quantum devices.

Several techniques are currently used to assess noise in qubits. Coulomb blockade oscillations of a "tuned-up" dot—a part of a spin qubit—provide a mechanism for measuring charge noise near the qubit but only at low frequencies, below ~1000 Hz. At 1-10 MHz, an operational qubit can study noise through gate operations [4, 5,6]–but this requires intensive experiments lasting months-to-years per device and requires a large investment of time and effort. Consequently, sufficient statistical information about relevant charge defects is lacking.

In field of SC qubits, much has been accomplished by using resonators to probe the degradation of Q at low power levels [2]. Here, we attempt to extend this technique by measuring noise spectra from materials useful for both types of semiconductor qubits.

1.1. TLS defects

The defect states that limit solid state qubits are believed to be two-level-systems/two-level-fluctuators (TLS) which are defects that occur at surfaces, interfaces, and in bulk materials. The exact microscopic nature of TLS is unknown, but they are modeled with a double well potential as shown in Figure 1. The two wells of the potential are slightly offset in energy leading to a ground state and an excited state separated by a barrier high enough to keep the states distinct. Typically, such defects couple energy through the electric fields in the qubits and decay via emission of phonons. This model suggests the TLS have a dipole moment that couples to electric fields. The difference in energy of the two states can vary widely depending on the details of the barrier and the energy difference of the well minima. This leads to a broad distribution of TLS energies which are believed to be flat or "white" to frequencies much higher than the ~10 GHz used by qubits [7].

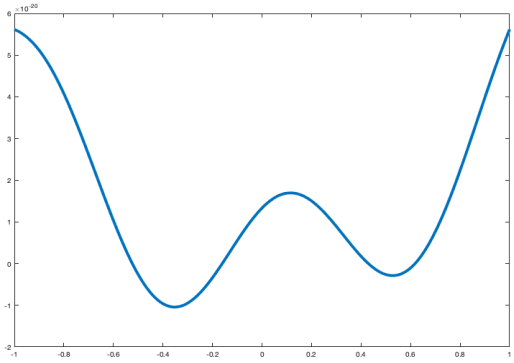

Figure 1. Double well potential model of TLS

The coupling of the qubit to the TLS is simply that of a dipole to an electric field.

$$g \approx \overrightarrow{d} \cdot \vec{E}$$

Here, **g** is the coupling energy, **d** is the dipole moment of the TLS and **E** is the electric field due to the qubit. The TLS are expected to occur with all possible orientations—they are not tied to the lattice since they occur at surfaces and in amorphous dielectrics. However, qubits do have preferred orientations of the electric field and so there is also considerable natural variation in the strength of qubit-to-TLS couplings. In spin qubits, which do not have an electric field associated with the quantum state, the effects of TLS are more evident in confinement and readout as charge fluctuations cause problems for both. Also, various mechanisms exist, for example, spin orbit coupling, which weakly couple spins to electric fields [8]. Both valley degeneracy [9,10] and stark shifts [11] have also been shown to couple spin to electric fields.

The TLS have a deleterious effect on qubits, as they provide a "decay path" for energy. In the quantum world, where a qubit only contains a single quantum of energy, any decay path leads to rapid loss of the qubit state and hence decoherence. Thus, it is highly desirable to understand TLS defects more thoroughly and understand how to build quantum circuits with lower densities of TLS defects.

A primary goal of this project has been to develop a new tool—noise measurements—as a means for looking at the TLS system.

1.2. Superconducting Resonators

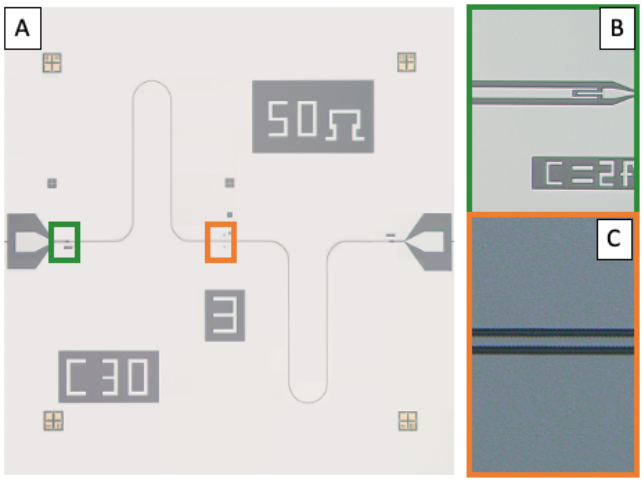

Figure 2. Overview of Coplanar Waveguide (CPW) resonator chip.

Figure 2 shows a coplanar waveguide (CPW) resonator fabricated for this project. The resonator is formed by a ~11.4 mm long section of CPW transmission line interrupted by 2 gaps form coupling capacitances. This creates a $\lambda/2$ resonant cavity. Figure 2A. shows the whole chip which is 5.95 mm on a side. An example of a coupling capacitance is shown in Fig. 2B. The approximately 2 fF capacitance has a 20 μm long finger. Fig. 2C shows the ground-signal-ground configuration of the CPW line. The ground and signal (lighter color) are e-beam deposited aluminum, approximately 100 nm thick. The gaps between the signal and grounds (darker) are bare silicon. The device pictured in Fig. 2 has a 3 μm wide signal line with 2 μm gaps to the ground planes.

All the resonators examined during this project used aluminum as the superconductor. Different substrates with different oxidation conditions were also examined and are detailed in table 1.

Microwave frequency resonators have frequencies in the same range (GHz) as qubits and couple to TLS through dipole-electric field interactions as described above. Transmission line resonators are easy to fabricate in a single photolithography step. When superconducting metals are used, transmission line resonators can have high Qs. This project created ~ 4.5 GHz resonators with linewidths of about 57 kHz or Q = f_r/fwhm= 80k. Here fwhm is the full width at half maximum of the resonant curve. This was mostly limited by the coupling capacitances into and out of the resonator.

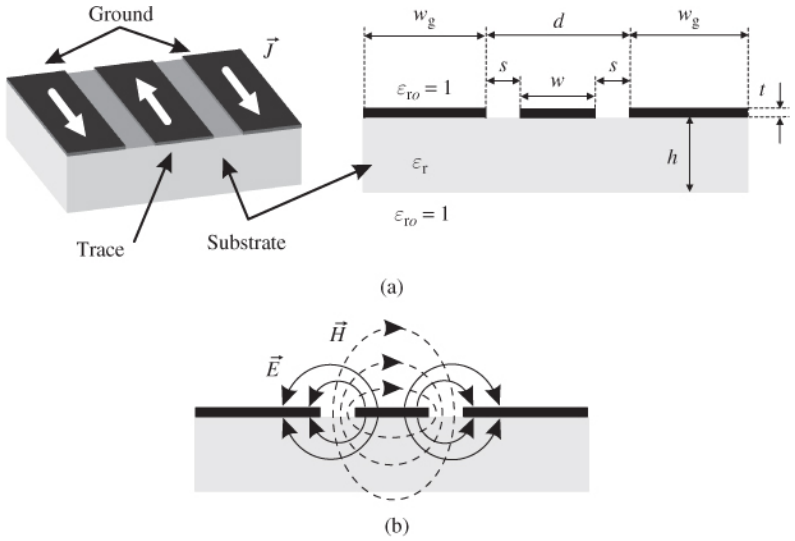

Figure 3. Details of CPW transmission lines

Figure 3 gives more details on the CPW geometry. CPWs are used here because the electric field in this design is roughly planar and the design can be fabricated in a single lithography step. Further, the CPW transmission line resonators are long—the resonators measured here are typically more than 11 mm in length—and so wind across a whole chip, sampling a representative cross section. The electric field strength in the CPW is a function of the impedance and the gap between the signal line and ground planes. Several of these resonators featured narrow gaps to increase the electric field strength and therefore the interaction with TLS.

1.3. Noise measurements

TLS couple to the electric field in the resonator creating state dependent change in its reactance [12]. Each TLS thus produces a state dependent frequency shift $\Delta f = g^2 \left|\frac{1}{(f_r - f_{tls})}\right|$ where f_r is the frequency of the resonator, f_{tls} is the frequency of the TLS, and g is a coupling constant that incorporates the strength of the electric field and the orientation of the TLS in that field among other factors. The effect of the TLS on the resonant frequency is analogous to the effect of a qubit in a circuit quantum-electrodynamics (cQED) measurement [13, 14]—the TLS pulls or pushes the

resonant frequency slightly higher or lower. A bath of TLS with frequencies near the resonator frequency thus produces a random walk in the resonant frequency over time as coupled TLS states flip transition back and forth.

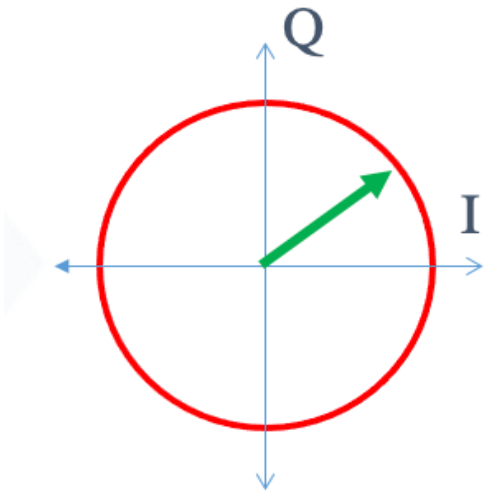

Figure 4. Illustration of the I Q plane

The experiment is performed by supplying microwave photons on resonance to the cold resonator and then detecting them after passage through the resonator, the microwave equivalent to a Michelson interferometer [15]. Detection was performed using an IQ mixer operated in a homodyne configuration. The outputs of the mixer are DC voltages which depend on the amplitude of the returning signal and upon the noise imparted upon. Analysis is performed in the IQ plane as in Fig. 4. If the local oscillator at the detector is detuned from the returning signal (making the measurement heterodyne), I and Q describe a vector which precesses around the origin forming a circle whose radius is proportional to the amplitude of the detected signal. If the local oscillator

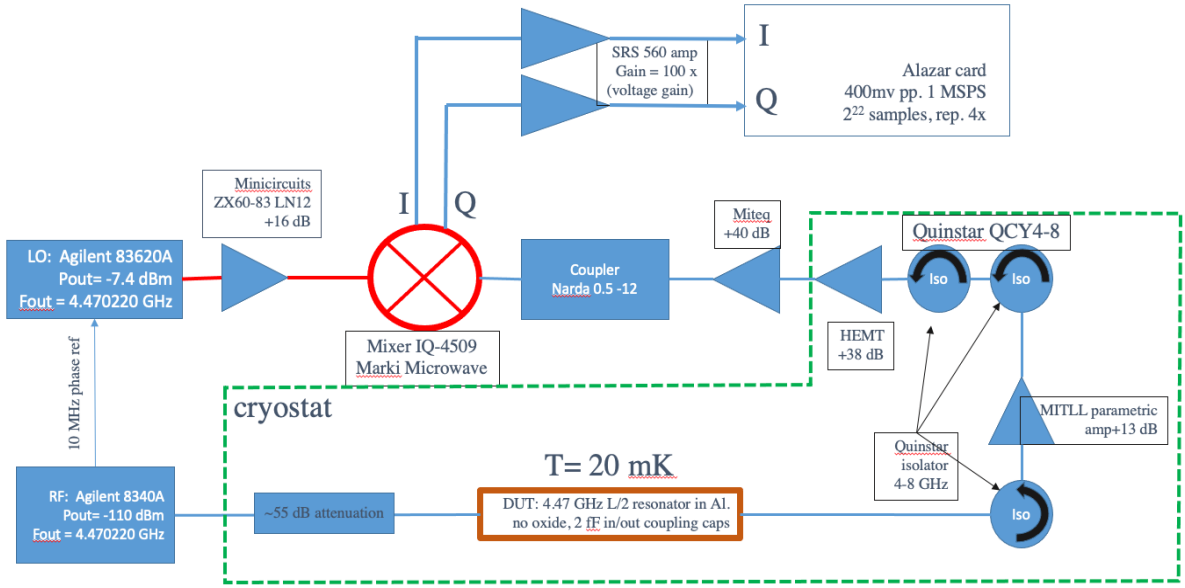

Figure 5. Schematic representation of the measurement. Items inside the green dashed line are inside the cryostat.

frequency matches the returning signal (homodyne detection) I and Q form a vector at a fixed angle. After digitizing I and Q, this vector is rotated to be along the I axis. Fluctuations in the amplitude of the signal—for instance due to fluctuations in the number of photons present in the resonator—cause the signal strength to increase/decrease. These effects are seen in the I channel. Small fluctuations in the phase of the signal—due to changes in the resonant frequency—show up as voltage in the Q channel. The random walk of the resonator in frequency produces noise almost entirely in the Q channel and is phase noise [12]. It is these small changes in phase that this experiment hopes to see.

Figure 5 gives details on the experimental setup for the measurement. The samples are cooled in a dilution refrigerator to about 20 *mK*. The low temperature is necessary so that TLS states decay through phonon emission instead of being thermally occupied. This also dictates the resonant frequency of the sample resonators which needs to be larger than the ambient temperature to achieve low thermal occupation of the resonator and control the number of photons. Expressed in symbols, $f_r > k_B T/h$ where k_B is Boltzmann's ($1.38 \cdot 10^{-23}$) constant and h Planck's constant ($6.626 \cdot 10^{-34}$) and T is temperature. In our experiments, we chose resonators mostly between 4.5 *GHz* and 5.5 *GHz*. The temperature equivalents at these frequencies are 200 *mK* and 300 *mK* respectively, indicating that at 20 *mK* low (<1) thermal occupation of the microwave photon modes can be achieved.

Table 1. summarizes details of all the resonators tested for this project.

Table 1. Summary of resonators tested

Device ID	Device type	f_{res} (GHz)	Q_t (high power)	Qc	Coupling capacitors	Oxide	Geometry C:G
A	λ/2 on Si	5.5	1200	1.4k	7fF/18fF	Native	10 : 6 um
B	λ/4 on SOI	3.6	28k	-	-	native	
C	λ/2 on Si	4.5	78k	100k	2fF/2fF	None (BOE)	3:2 um
D	λ/2 on Si	4.5	39k	43k	3fF/3fF	Native	3:2 um
E	λ/2 on Si	-	failed	~40k	3fF/3fF	750C oxide	3:2 um
F	λ/2 on Si	-	failed	~40k	3fF/3fF	1050C oxide	3:2 um

2. WHAT WAS LEARNED

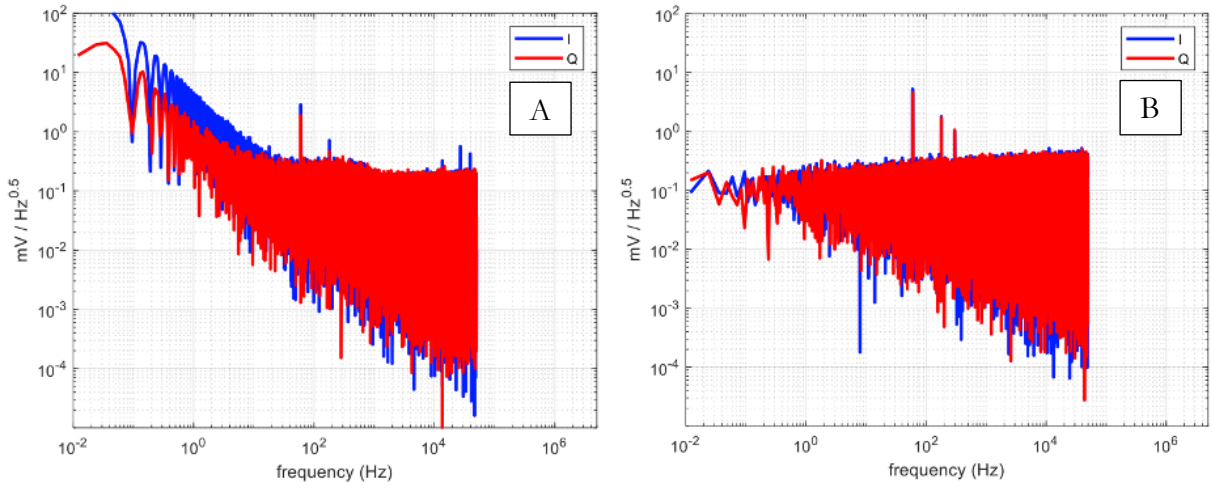

Figure 5. Noise spectra recorded for sample C at 22 *mK* for both high (A) and low power (B) conditions.

Figure 5 shows the results of two noise measurements. These data were collected on C in table 1 which is a 4.5 GHz λ/2 mode transmission line resonator with a 3 μm signal line and 2 μm gaps to ground deposited on a high resistivity float zone silicon wafer. The sample was dipped in a buffered oxide etch (BOE) prior to metal deposition to remove the native oxide from the silicon substrate. The resonant line width (full width at half maximum) of this resonator at high power (many photon) limit was about 57 kHz and degraded to about 70 kHz in the low power (single photon) regime. Also note the frequency resolution of the microwave generators used in these experiments are better than 1 Hz, much finer than the resonant linewidths. Other salient details include the sample temperature of 22 *mK* and the measurement power which was varied.

Both data in Figure 5 were acquired while injecting microwave photons on resonance into the resonator. Fig. 5A was measured when the injected microwave signal was less than -157 dBm of microwave power at the resonator input port, corresponding to approximately single photon occupation of the resonator. The data in Fig. 5B were acquire at moderate power of -115 dBm or ~ 10^4 photons in the resonator. The second curve shows a significant 1/f character over nearly 4 orders of magnitude and up to nearly 100 Hz.

However, it is difficult to separate the contributions of the sample from the contributions of the measurement chain. Further calibration is needed. Also, the noise is nearly equally present in both I and Q channels. As discussed above, noise due to TLS should be mostly only present in the Q channel [12].

3. CONCLUSIONS

Unfortunately, the results are inconclusive. It is difficult to distinguish whether noise is due to TLS in the experiment or due to 1/f noise in the amplifier chain. Further calibration of the amplifier chain, mixer, and other detector components is needed to isolate these sources of noise.

REFERENCES

[1] B.E. Kane, A silicon-based nuclear spin quantum computer ", *Nature*, **393 (1998)**.

[2] John M. Martinis, K.B. Cooper, R. McDermott, Matthias Steffen, Markus Ansmann, K. Osborn, K. Cicak, S. Oh, D.P. Pappas. R.W. Simmonds, Clare C, Yu, Decoherence in Josephson Qubits from Dielectric Loss**,** Phys. Rev. Lett. **95**, 210503 (2005).https://journals.aps.org/prl/abstract/10.1103/PhysRevLett.95.210503

[3] Dieter K. Schroder, 'Semiconductor Material and Device characterization, Third Edition,' John Wiley and Sons, Inc., 2006.

[4] O. E. Dial, M. D. Shulman, S. P. Harvey, H. Bluhm, V. Umansky, and A. Yacoby, 'Charge Noise Spectroscopy Using Coherent Exchange Oscillations in a Singlet-Triplet Qubit', Phys. Rev. Lett. 110, 146804 (2013).

[5] J. Yoneda, K. Takeda, T. Otsuka, T. Nakajima, M. R. Delbecq, G. Allison, T. Honda, T. Kodera, S. Oda, Y. Hoshi, N. Usami, K. M. Itoh, and S. Tarucha, 'A quantum-dot spin qubit with coherence limited by charge noise and fidelity higher than 99.9%,' Nat. Nanotechnol. 13, 102 (2018).

[6] Chan, K. W. , Huang, W., Yang, C. H., Hwang, J. C. C., Hensen, B. , Tanttu, T., Hudson, F. E. , Itoh, K. M. , Laucht, A., Morello, A. and Dzurak, A. S., 'Assessment of a Silicon Quantum Dot Spin Qubit Environment via Noise Spectroscopy,' Phys. Rev. Applied 10, 4 044017, (2018).

[7] M. v. Schickfus and S. Hunklinger, Phys. Lett. A64, 144(1977).

[8] Ryan M. Jock , N. Tobias Jacobson, Patrick Harvey-Collard, Andrew M. Mounce, Vanita Srinivasa, Dan R. Ward, John Anderson, Ron Manginell, Joel R. Wendt, Martin Rudolph, Tammy Pluym, John King Gamble, Andrew D. Baczewski, Wayne M. Witzel, and Malcolm S. Carroll, 'A silicon metal-oxide-semiconductor electron spinorbit qubit', Nature Comm. 9, 1768 (2018); DOI: 10.1038/s41467-018-04200-0

[9] Dimitrie Culcer, Xuedong Hu, and S. Das Sarma, 'Dephasing of Si spin qubits due to charge noise', Appl. Phys. Lett. 95, 073102 (2009); https://doi.org/10.1063/1.3194778.

[10] John King Gamble, Patrick Harvey-Collard, N. Tobias Jacobson, Andrew D. Baczewski, Erik Nielsen, Leon, Maurer , Inès Montaño, Martin Rudolph, M. S. Carroll, C. H. Yang, A. Rossi, A. S. Dzurak, and Richard P. Muller,'Valley splitting of single-electron Si MOS quantum dots', Appl. Phys. Lett. 109, 253101 (2016); https://doi.org/10.1063/1.4972514

[11] Chan, K. W. , Huang, W., Yang, C. H., Hwang, J. C. C., Hensen, B. , Tanttu, T., Hudson, F. E. , Itoh, K. M. , Laucht, A., Morello, A. and Dzurak, A. S., 'Assessment of a Silicon Quantum Dot Spin Qubit Environment via Noise Spectroscopy,' Phys. Rev. Applied 10, 4 044017, (2018).

[12] Jiansong Gao, Jonas Zmuidzinas, Benjamin A. Mazin, Henry G. LeDuc, and Peter K. Day, 'Noise Properties of Superconducting Coplanar Waveguide Microwave Resonators,' Appl. Phys. Lett. 90, 102507 (2007); https://doi.org/10.1063/1.2711770

[13] Jens Koch, Terri M. Yu, Jay Gambetta, A. A. Houck, D. I. Schuster, J. Majer, Alexandre Blais, M. H. Devoret,S. M. Girvin, and R. J. Schoelkopf, 'Charge-insensitive qubit design derived from the Cooper pair box', Phys. Rev. A 76, 042319 (2007) https://journals.aps.org/pra/abstract/10.1103/PhysRevA.76.042319

[14] A. A. Houck, Jens Koch, M. H. Devoret, S. M. Girvin, R. J. Schoelkopf, Life after chare noise: recent results with transmon qubits, Quant. Inf. Proc. 8, 105 (2009); DOI: 10.1007/s11128-009-0100-6

[15] Albert Michelson; Edward Morley (1887). "On the Relative Motion of the Earth and the Luminiferous Ether". American Journal of Science. 34 (203): 333–345. Bibcode:1887AmJS...34..333M. doi:10.2475/ajs.s3-34.203.333. S2CID 124333204.

DISTRIBUTION

Email—Internal

Name	Org.	Sandia Email Address
Art J. Fischer	1879	ajfisch@sandia.gov
Tom Harris	1882	ctharri@sandia.gov
Sueli Skinner-Ramos	1882	sdskinn@sandia.gov
Will Kindel	5219	wkindel@sandia.gov
Technical Library	01977	sanddocs@sandia.gov

This page left blank

This page left blank

Sandia National Laboratories

Sandia National Laboratories is a multimission laboratory managed and operated by National Technology & Engineering Solutions of Sandia LLC, a wholly owned subsidiary of Honeywell International Inc. for the U.S. Department of Energy's National Nuclear Security Administration under contract DE-NA0003525.